Saudi Pharmaceutical Journal 27 (2019) 584–592

Contents lists available at ScienceDirect

Saudi Pharmaceutical Journal

journal homepage: www.sciencedirect.com

Original article

Synthesis, characterization and cytotoxic activity of naturally isolated naringin-metal complexes

Emad M. Atta [a,b,*], Khaled H. Hegab [a,c], Ahmed A.M. Abdelgawad [a,d], Abdelghany A. Youssef [a,e]

[a] Chemistry Dept., Faculty of Science, Jazan Univ., Saudi Arabia
[b] Genetic Engineering and Biotechnology Research Institute Univ. of Sadat City, Egypt
[c] Inorganic Chemistry Dept. National Research Center, Giza, Egypt
[d] Medicinal and Aromatic Plants Dept., Desert Research Center, Cairo, Egypt
[e] Medicinal and Aromatic Plants Researches Dept., Pharmaceutical and Drug Industries Division, N. R. C., Giza, Egypt

ARTICLE INFO

Article history:
Received 24 September 2018
Available online 13 February 2019

Keywords:
Naringin (HL)
Isolation
Citrus maxima
Ag(I), Y(III) and Ru (III) ligand complexes
Anticancer

ABSTRACT

High-purity naringin was isolated from the fruit peels of *Citrus maxima and* characterized by various spectroscopic methods like UV and NMR. The isolated compound ligand (HL) was used as ligand-metal complexes synthesis after using Ag (I), Y (III) and Ru (III) metals. These ligand-metal complexes were characterized by elemental analysis, FT-IR, UV–VIS, TGA, molar conductance and magnetic properties. Cytotoxic activity of the isolated naringin and its metal complexes were investigated against two human cancer cell lines namely, white breast Adenocarcinoma (MCF7) and Lung carcinoma (A549) using cell viability assay. Transition metal increased the cytotoxic activity of naringin when they were conjugated. LC50 of Ag ligand complex demonstrated strong cytotoxicity against MCF-7 and A549 cell line that was found higher active more than three and four times the strength, respectively when compared to LC50 of Adriamycin. While LC50 of Adriamycin compound was slightly more active only about 30% and twice the strength of the Ru ligand complex against MCF-7 and A549 cell line, respectively.

1. Introduction

Natural resources including plants and their extracts have been used in folk medicine for the treatment of many diseases (Ghazanfar, 1994; Vishnu Varthan et al., 2013). Metal complexes play an essential role in medicine and in agriculture (Agrawal, 2015). Metal complexes of Schiff bases possess anti-inflammatory, anti-allergic, antioxidant and analgesic, antifertility, enzymatic (Sing et al., 1999), antiproliferative (Ejidike and Ajibade, 2016) antiviral (Agrawal, 2015), and antimicrobial activity (Vasile Scăeţeanu et al., 2018; Obasi et al., 2017).

The biological activity of flavonoids compounds had supposed to increase if these natural compounds were coordinated with transition metal ions. Transition metal complexes based on flavonoid ligands have been investigated (Pereira et al., 2007; Al Hassani et al., 2015; Jun et al., 2007). Complexes like rutin-Fe (II) and rutin-Cu (II) have demonstrated higher biological activity as antioxidants and anti-inflammatory than free rutin (Afanasév et al., 2001; Hynes and O'Coinceanainn 2004; Pereira et al., 2007). The literature revealed that naringin-derived copper (II) complex, shows higher anti-inflammatory and antioxidant activity when compared with naringin alone (Pereira et al., 2007).

Citrus maxima (J. Burm.) Merr. is extensively distributed all over the world. It is also called pumelo or shaddock which belongs to the *Rutaceae* family (citrus family). Naringin is the main flavonoid compound present in *Citrus maxima*. It is responsible for the physiological properties of grapefruit and orange juice (Gorinstein et al., 2006; Kanaze et al., 2003). Naringin metal complexes were discussed in many studies in the last decade (Hynes and O'Coinceanainn, 2004; Zhang and Brodbelt, 2005; Mello et al., 2007; Rout et al., 2013).

Cancer is a serious life-threatening disease that is increasingly prevalent in many countries around the world (Ibrahim et al., 2008). The therapeutic use of metal complexes in cancer and leukemia are reported from the sixteenth century (Agrawal, 2015). Complexes formed with metals like Cu, Au, Ga, Ge, Sn, Ru, Rh, Ir

* Corresponding author at: Chemistry Depart. Fac. of Science, Jazan Univ. Jazan, P. O. Box 114, Saudi Arabia.
E-mail address: emadata@yahoo.com (E.M. Atta).
Peer review under responsibility of King Saud University.

Production and hosting by Elsevier

https://doi.org/10.1016/j.jsps.2019.02.006
1319-0164/

was shown significant antitumor activity in animals (Knoll and Turro, 2015).

Therefore, this work attribute isolation and purification of naringin from *Citrus maxima* and the synthesis of Ag(I), Y (III) and Ru (III) transition metals complexes bearing a naringin compound. These compounds were successfully characterized by Nuclear Magnetic Resonance (NMR), FT-IR, UV–VIS, mass spectrometry and elemental analysis. Further these ligand metal complexes will apply for the cytotoxic activity in human cancer cell lines like Adenocarcinoma (MCF7) and Lung carcinoma (A549).

2. Experimental

2.1. Chemical and instruments

All melting points were measured using a Büchi 510 melting point apparatus and are reported uncorrected. The IR spectra (4000–400 cm^{-1}) were measured using KBr pellets in a Jasco FT/IR 300E Fourier transform infrared spectrophotometer and in the 500–100 cm^{-1} region using Polyethylene-Sandwiched Nujol mulls on a Perkin Elmer FT-IR 1650 (spectrophotometer). Elemental analyses were performed at the Micro analytical Laboratory of the National Research Centre. Molar conductance was measured at room temperature on electronic conductivity model 19000-05 (USA). The electronic absorption spectra were recorded using a Shimadzu UV-240 UV–Visible recording spectrometer. Thermogravimetric analyses were measured using a DTA-7 and TGA-7 Perkin Elmer 7 series thermal analyses system. The magnetic moments were measured using Gouy method with Hg [Co $(SCN)_4$] as calibrate. The metal content of the complexes was determined by complex-metric titration after decomposition with acid. Thin-layer chromatography silica-gel alumina sheet-Merck 60 F_{254} pre-coated sheets have tested the purity of synthesized compounds.

All chemicals, solvents and metal salts ($AgNO_3$ (99%), Yttrium (III) chloride-Hexahydrate (99.99%) and Ruthenium (III) chloride (98%)) were purchased from Aldrich Chemical Co, USA and were used as received.

2.2. Plant materials

The Fruits of *Citrus maxima* was purchased from Panda hypermarket in Jizan city (Saudi Arabia) on March 2017. Fresh peels were fragmented with a food processor, whilst the skins were dried using an oven at 45 °C until a constant weight and then were powdered in a mortar and sieved.

2.3. Extraction, isolation and characterization of naringin

Naringin compound was extracted from the fruit peel of *Citrus maxima* according to Sudto et al. (2009) with some prior experimental modifications. Fifty grams of the dry powdered peel was macerated in methanol (500 mL) for 3 days. The slurry was filtered and the obtained methanol extract was dried with a rotatory evaporator under reduced pressure at 45 °C. The dry extract was subjected to further naringin isolation using water extraction/crystallization with dichloromethane addition method.

Water (60 mL) was added to the dry methanolic extract (10 g) and the obtained mixture was stirred at 70 °C for 30 min before being transferred into a separating funnel. Dichloromethane (10 mL) was added and the mixture was swirled and left for 3–4 days at 25 °C to allow crystallization of naringin in the aqueous layer. Finally, the naringin crystals collected by filtration through filter paper and air-dried.

The collected naringin was applied to thin layer chromatography (TLC) on silica gel using solvent systems (ethyl acetate: methanol: water (30:5:4 v/v/v), chloroform/acetone (4:1 v/v) and Dichloromethane: Methanol (8:2 v/v) for checking the purity of the isolated compound. The developed chromatograms were visualized under UV light at 240 and 366 nm. Then exposed to ammonia vapor and immediately re-examined to observe possible changes that may eventually appear in color or fluorescence. The separated material was purified by fractionation then subjecting to a Sephadex LH-20 column using methanol and water as eluting system. Structure of naringin was confirmed by comparison of R_f values on TLC and PC with authentic sample and by UV, ^{1}H NMR, and ^{13}C NMR spectral data.

Naringin: White needle crystals; mp 166–168 °C. FT-IR (KBr) 3423, 2927, 1641 cm^{-1}. ^{1}H NMR (acetone- d_6, δ, ppm): naringenin 2.73 (1H, d, J = 14.0 Hz, H-3a), 3.22 (1H, dd, J = 14, 17.6 Hz, H-3b), 5.32 (1H, d, J = 12.8 Hz, H-2), 6.13 (1H, s, H-6), 6.16 (1H, s, H-8), 6.81 (2H, d, J = 8.4 Hz, H-3′, 5′) and 7.31 (2H, d, J = 8.4 Hz, H-2′, 6′); glucose 5.09 (1H, d, J = 7.2 Hz, H-1″), 3.37–3.85 (6H, d, glucose protons); rhamnose 5.24 (1H, s, H-1‴), 1.27 (3H, d, J = 6.4 Hz, H-6‴) and 3.37–3.92 (4H, m, rhamnose protons). ^{13}C NMR (acetone-d_6, δ, ppm): Naringenin 44.4 (C-3), 81.0, (C-2), 96.8 (C-8), 97.9 (C-6), 105.5 (C-10), 116.37 (C-3′, 5′), 129.1 (C-2′,6′), 131.5 (C-1′), 157.9 (C-4′), 162.7 (C-9), 163.1 (C-5), 168.1 (C-7) and 197.1 (C-4); Glucose 61.3 (C-6″), 71.2 (C-4″), 77.4 (C-5″), 78.6 (C-3″), 79.8 (C-2″) and 99.0 (C-1″); rhamnose 18.3 (C-6‴), 69.2 (C-5‴), 71.8 (C-3‴), 72.2 (C-2‴), 73.7 (C-4‴) and 100.5 (C-1‴). MS (m/z): Cal. for C_{27} O_{14} H_{32} (580.18); found 603.17 $[M-Na]^+$. UV–Vis λ max, nm: (MeOH) 281, 327, 233, 213; ($AlCl_3$); (HCl); (NaOAc); (HBO_3). Anal. for **$C_{27}O_{14}H_{32}$ (580.18)**: calcd.: C, 55.81; H, 5.51. Found: C, 55.76; H, 5.49%.

2.4. Synthesis and characterization of Naringin-metal complexes

General methods: The Naringin-metal complexes were synthesized by adding a methanolic solution of metal salt (1 mmol in 10 mL methanol) to a solution of naringin (1 mmol in 5 mL methanol) dropwise with continuous stirring. The mixture was then refluxed for 3–6 h. The solution was concentrated. The precipitated product was obtained which was filtered and washed with cold ethanol and diethyl ether then dried in the vacuum desiccators over anhydrous calcium chloride. The structure of complexes was characterized by UV–Vis, FT-IR, TGA and elemental analysis. Metal salts were used namely, $AgNO_3$, $YCl_3{\cdot}6H_2O$ and $RuCl_3$. The metal content of the complexes was determined by complex -metric titration after decomposition with acid.

2.4.1. $[Ag(L)(H_2O)_2].4H_2O$ complex

Yield: 66.75%, 0.5 g pure, m.p. 253–255 °C. UV–Vis (MeOH) λ_{max}, nm: 335, 281, 225, 215. IR (KBr)ν/cm^{-1}: 3424, 3386, b ν (OH)H_2O, 2982ν (OH), 1727ν (C═O), 560 (Cu—O) cm^{-1}, molar conductance Λ_m ($\Omega^{-1}cm^2mol^{-1}$) = 21 (non-electrolyte), magnetic moment: 0.00 B. M (tetrahedral geometry). Anal. for **$C_{27}H_{43}O_{20}Ag$ (794.7):** Calc.: C, 40.77; H, 5.41; Ag, 13.55. Found: C, 40.70; H, 5.39; Ag, 13.49%.

2.4.2. $[Y(L)(H_2O)_2Cl_2].2H_2O$ complex

Yield: 73.19%, 0.56 g pure, m.p. 265–267 °C. UV–Vis (MeOH) λ_{max}, nm: 323, 283, 210. IR (KBr) ν/cm^{-1}; 3393, bν (OH)H_2O, 2977ν(OH), 1629ν(C═O), 538 (Y—O), 423 (Y-Cl) cm^{-1}, molar conductance Λ_m ($\Omega^{-1}cm^2mol^{-1}$) = 28 (non-electrolyte), magnetic moment: 0.00B.M (octahedral geometry). Anal. for **$C_{27}H_{39}O_{18}Cl_2Y$ (810.9)**: calcd.: C, 40.77; H, 4.90; Y^{+3}, 10.96. Found: C, 40.70; H, 4.85; Y^{+3}, 10.90%.

2.4.3. $[Ru(L)(H_2O)_2Cl_2].5H_2O$ complex

Yield: 76.14%, 0.60 g pure, M.p. > 300 °C. UV–Vis (MeOH) λ_{max}, nm: 333, 282, 224, 212, 534. IR (KBr)ν/cm^{-1}: 3386, b ν(OH)H_2O, 2972 ν(OH), 1627 ν(C═O),427 (Ru—O), 422 (Ru-Cl) cm^{-1}, molar conductance Λ_m ($\Omega^{-1}cm^2mol^{-1}$) = 25 (non-electrolyte, magnetic moment: 5.73 B.M (octahedral geometry). Anal. calcd. for **$C_{27}H_{45}O_{21}Cl_2Ru$ (877.7):** C, 36.91; H, 5.12; Ru^{+3}, 11.58. Found: C, 36.87; H, 5.10; Ru^{+3}, 11.50%.

2.5. In-vitro anticancer activity using cell line assay

In-vitro anticancer ability of naringin isolated from *Citrus maxima* and its metal complexes were investigated against human breast adenocarcinoma (MCF7) and Lung carcinoma cell line (A549). Cells viability of MCF7 and A549 was assessed by MTT assay [3-(4,5-dimethylthiazol-2-yl)-2, 5-diphenyl tetrazolium bromide] which is based on mitochondrial dependent reduction of yellow to purple formazan (Mabry et al., 1970). Cells were suspended in RPMI 1640 medium. All samples were tested with different concentrations as 100, 50, 25, 12.5, 6.25, 3.125, 1.56 and 0.78 μg/ml (Al Hassani et al., 2016; Sudhanshu et al., 2013). After 48 h of incubation, medium was aspirated, 40ul MTT salt (2.5 μg/ml) were added to each well and incubated for further four hours at 37 °C under 5% CO2. To stop the reaction and dissolving the formed crystals, 200 μL of 10% Sodium dodecyl sulphate (SDS) in deionized water was added to each well and incubated overnight at 37 °C. A positive control which composed of 100 μg/ml was used as a known cytotoxic natural agent who gives 100% lethality under the same conditions (Thabrew et al., 1997, and El-Menshawi et al., 2010). The absorbance was measured using a microplate multiwell reader (model 3350; Bio-Rad Laboratories Inc., Hercules, California, USA) at 595 nm and a reference wavelength of 620 nm. The percentage of change in viability was calculated according to the following formula:

((Reading of extract/Reading of negative control) − 1)x100

A probit analysis was carried for IC_{50} and IC_{90} determination using SPSS 11 program.

The cytotoxic of metal salts did not investigated alone that in most cases precipitation was observed in case of the silver pillarplexes as well as for AgNO3 and AuCl3 (Pöthig et al., 2018). Also, on Ru metal (Corrêa et al, 2016).

3. Results

3.1. Isolation, purification and characterization of the naringin

Naringin compound was extracted from the fruit peel of *Citrus maxima* was according to Sudto et al., (2009) with some prior experimental modifications. Isolated naringin which was obtained from the aqueous layersubjected to TLC using eluent system ethyl acetate: methanol: water in ratio 30:5:4; It was found that, the naringin is not completely pure and contains other flavonoid compounds. The precipitate was applied to successive fractionation by separating funnel using acetone and ethyl acetate from the aqueous solution. Naringin purity was further checked by thin layer chromatography (TLC). Finally, the purified naringin was obtained from the Sephadex column and checked for purity with standard naringin sample (Sigma Aldrich, Naringin: N1376-25G) to get the accurate rate of flow of naringin (R_f = 0.53 in ethyl acetate: methanol: water (30:5:4); R_f = 0.62 in methanol: water: acetic acid (50:44:6); R_f = 0.45 in Dichloromethane: Methanol (8:2). The pure isolated ligand (HL) crystals (naringenin-7-*O*-neohesperidoside) was confirmed by UV–Vis., FT-IR, MS spectroscopy and ^1H, ^{13}C NMR, then by comparison with published data in Mabry et al., 1970 and Al-Obaidi, 2014.

3.2. Complexation and characterization

3.2.1. Molar conductance

The molar conductance and the elemental analyses data were revealed in Table 1. To establish the charge of the metal complexes at room temperature, were measured the molar conductivities of their solutions (10^{-3} M) as the metal complexes were dissolved in DMF and the molar conductance value of all complexes recorded in range 21–28 $\Omega^{-1}cm^2mol^{-1}$ indicates non-electrolytic nature of these complexes (Lucilene et al., 2007).

3.2.2. Infrared spectra

The IR spectral (Fig. 1) information of the Ligand **HL** and the prepared complexes were recorded in Table 2. IR spectrum of ligand HL for OH groups shows a broad band from 2927 to 3423 cm^{-1}, phenolic ν OH and sharp band of ν C═O at 1641 cm^{-1}. For all metal complexes which prepared show broad bands around 3424–3386 cm^{-1} assignable to ν (OH) of water molecules (Regina et al., 2007). The complexes Ag(I), Y(III) and Ru(III)-L exhibit a strong stretching band for phenolic ν OH at 2982, 2977 and 2972 cm^{-1}, respectively, indicating the shift of the band position to higher energy compared to the starting ν (OH) of the ligand, where ν OH is at 2927 cm^{-1} (Al-Obaidi, 2014; Abd-El-All et al., 2013). The complexes of Ag(I), Y(III) and Ru(III)-L exhibit a strong stretching band for ν C═O at 1727, 1629 and 1627 cm^{-1} respectively, indicating the shift of the band position compared to the starting carbonyl group of the ligand. Where ν C═O is at 1641 cm^{-1} (Munde et al., 2010) which emphasized the participation of the carbonyl group and phenolic OH group (in position 5 in A-ring- Fig. 4) in a coordinated bond with the metal ions. Also, in the IR spectra, the validation of this coordinated bond was detected, a new band in the complexes appeared at 484–560 cm^{-1}, this band was not found in the free ligand HL and was assigned to C═O—M bond (Al Hassani et al., 2015). Also, only in the choro complex, $[Y(L)Cl_2(H_2O)_2].2H_2O$, and $[Ru(L)Cl_2(H_2O)_2].5H_2O$ the band at 423 and 422 cm^{-1}, respectively, is attributed to ν (M—Cl) of the terminal bonded chloride ions (Lucilene et al., 2007).

3.2.3. Electronic spectra and magnetic moment:

The magnetic moment values, electronic absorption spectral (Fig. 2) of HL and its complexes data are shown in Table 3. Free naringin (HL) exhibits an absorption a very week band at 326 nm, corresponding to the B ring portion and maximum one in methanol solution at 282 nm, corresponding to the A ring portion (Saadiyah et al., 2012). In all prepared complexes, the intra-ligand and charge transfer bands were reported in the range 210–333 nm. The diamagnetic structure of Ag (I) complex was confirmed by zero magnetic moment. The obtained data confirm tetrahedral geometry around the Ag (I) ion (Abd-El-All et al; 2013; Mosmann, 1983). In addition, zero magnetic moment of Y (III) complex (diamagnetic character) confirmed octahedral complex around Y (III) ion. The octahedral geometry of Ru (III) ion in ligand complex is confirmed by the measured magnetic moment values at 5.73B. M, which is in harmony with the reported value and only d-d transition band at 534 nm (Lucilene et al., 2007).

3.2.4. Thermal gravimetric analysis TGA:

The formulae suggested from the analytical results and thermogravimetric analysis data showed good agreement Table 4. The TGA curve of $[Ag(L)(H_2O)_2].4H_2O$ complex: shows that in the first step, the first weight loss of 8.95 (cal. 9.06) from 70 to 120 °C and the second step, second weight loss of 4.5(cal.4.53)% from 120 to 220 °C, corresponds to the loss of two and four hydrated H_2O molecules, respectively. By increasing temperature, the third step, led to the more decomposition at range 220–800 °C for

Table 1
Analytical, physical and conductivity data for HL and their metal complexes:

Compound	M: L	M.p. (°C)	Caled (Found)%			Molar conductance ($ohm^{-1}cm^2mole^{-1}$)
			C%	H%	M%	
Ligand (HL) **$C_{27}H_{32}O_{14}$ (580.54)**	———	166–168	55.81 (55.76)	5.51 (5.49)	——————	———————
[Ag(L)$(H_2O)_2$]. 4H_2O $C_{27}H_{43}O_{20}Ag$ (794.7)	1:1	253–255	40.77 (40.70)	5.41 (5.39)	13.55 (13.49)	21
[Y(L)$(H_2O)_2$ Cl_2]0.2 H_2O $C_{27}H_{39}O_{18}Cl_2Y$ (810.9)	1:1	265–267	39.95 (39.89)	4.80 (4.75)	10.96 (10.90)	28
[Ru(L)$(H_2O)_2$ Cl_2]. 5H_2O $C_{27}H_{45}O_{21}Cl_2Ru$ (877.7)	1:1	300<	36.91 (36.87)	5.12 (5.10)	11.58 (11.50)	25

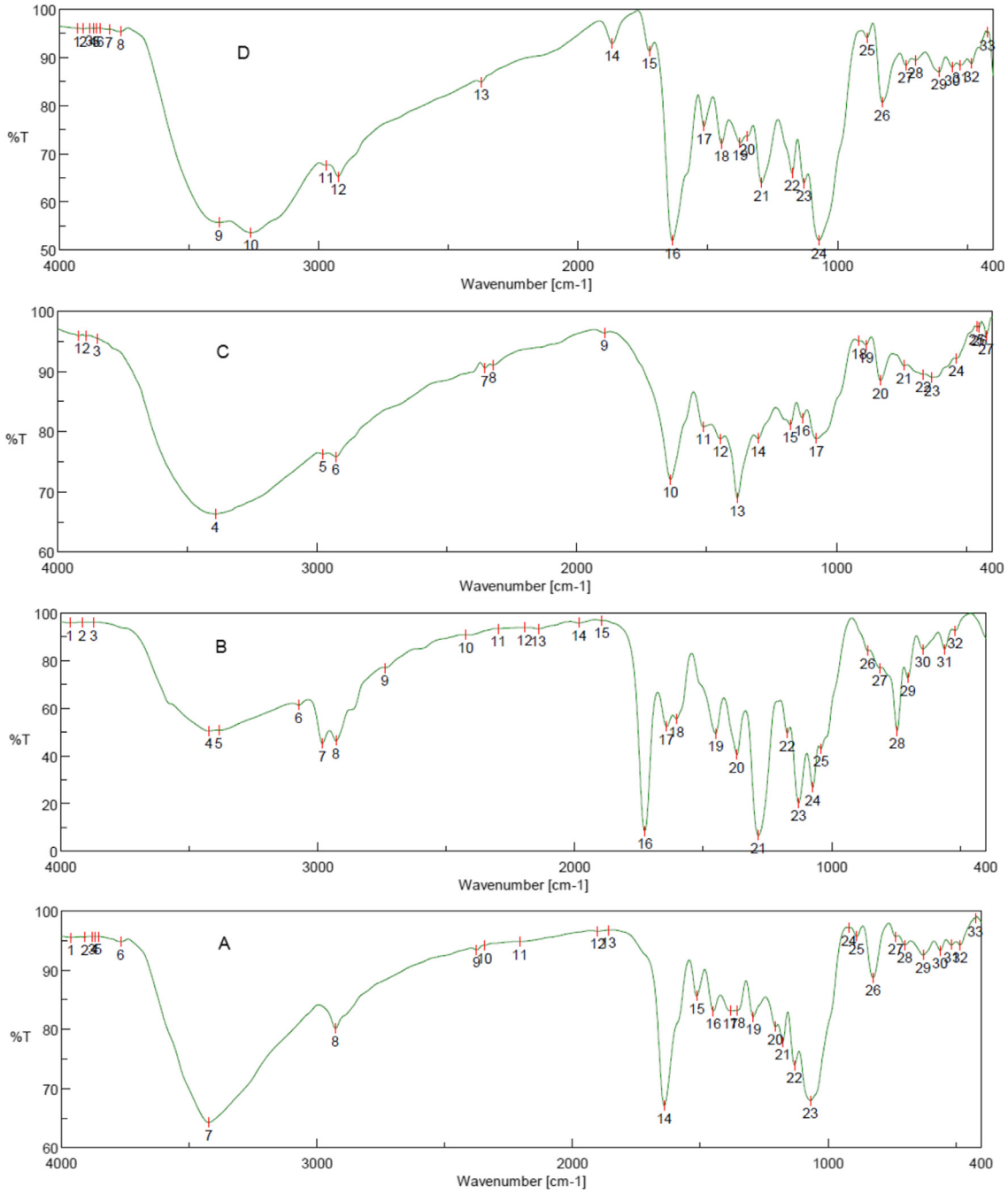

Fig. 1. IR spectra of the ligand **HL** and its prepared complexes [A: **HL**, B: Ag-**L**, C: Y- **L** and D: Ru-**L**)].

organic parts but at 1000 °C only remain silver metal as 13.5 (cal.13.55)%.

Also, The TGA curve of [Y(L)$(H_2O)_2Cl_2$].2H_2O complex: shows that in the first step, the first weight loss of 4.40 (cal. 4.44) from 50 to 100 °C. The second step, second weight loss of 13.58 (cal.13.19)% from 100 to 230 °C, corresponds to the loss of two molecules of hydrated water and two coordinated water molecules with two chlorine ions, respectively. By raising temperature, the

Table 2
Infrared spectral data for HL and its metal complexes.

Compound	ν_{H2O}	ν_{OH}	$\nu_{C=O}$	ν_{M-O}	ν_{M-Cl}
Ligand (HL)	————	3423,2927	1641	————	————
$[Ag(L)(H_2O)_2].\ 4H_2O$	3424,3386,b	2982	1727	560	————
$[Y(L)(H_2O)_2\ Cl_2]0.2\ H_2O$	3393,b	2977	1629	538	423
$[Ru(L)(H_2O)_2\ Cl_2].\ 5H_2O$	3386,b	2972	1627	484	422

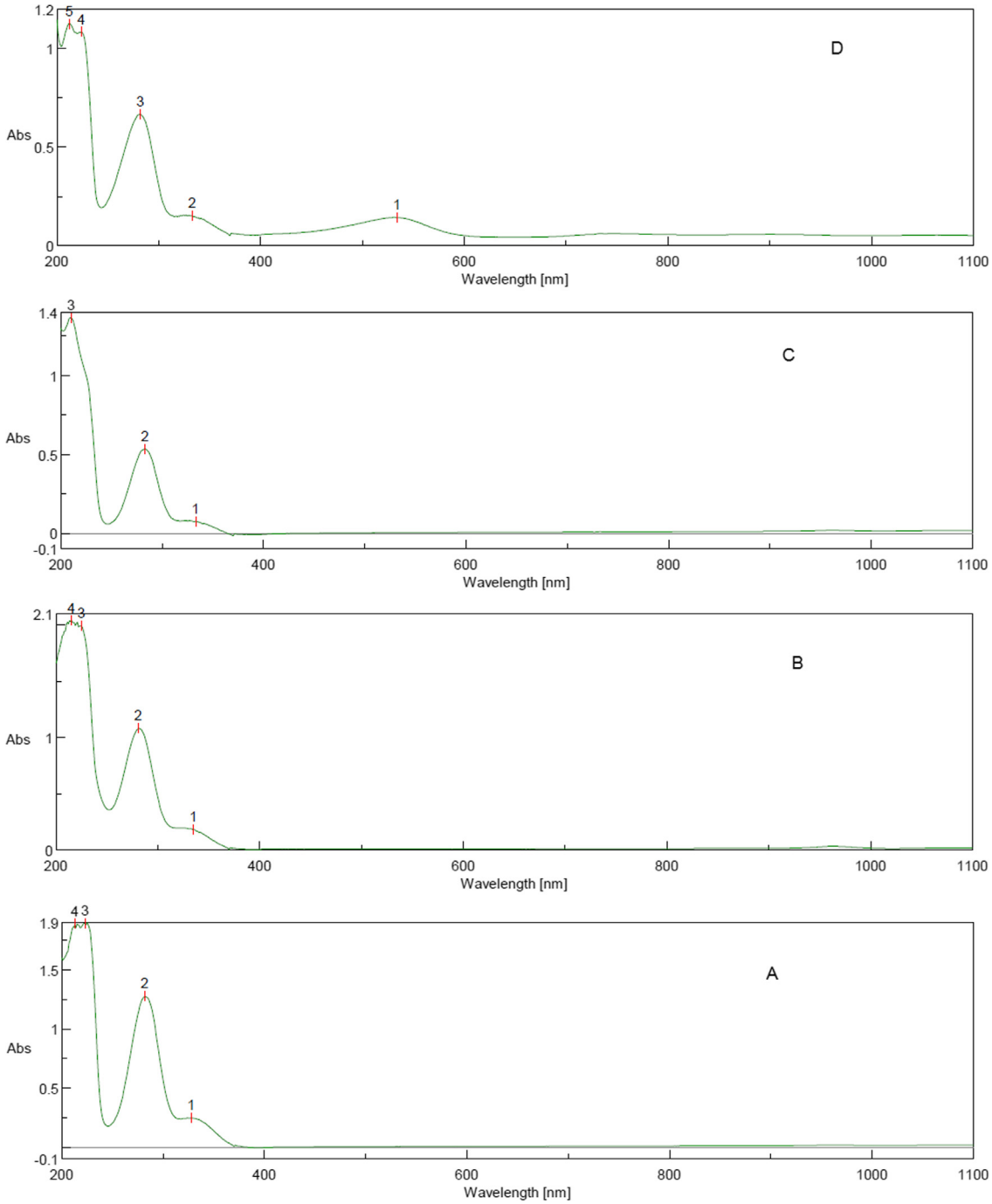

Fig. 2. Electronic spectra of ligand **HL** and its metal complexes. [A: **HL**, B: Ag-**L**, C: Y-**L** and D: Ru-**L**)].

third step, further decomposition at range 240–700 °C for organic parts but at 750 °C the Y_2O_3 is the final product remains stable as 27.69(cal.27.84)%.

Finally, The TGA curve of $[Ru(L)(H_2O)_2Cl_2].5H_2O$ complex: shows that in the first step, the first weight loss of 10.36 (cal.10.25)% from 50 to 140 °C. The second step, second weight loss of 12.26 (cal.12.19)% from 150 to 236 °C, corresponds to the loss of two molecules of hydrated water and two coordinated water molecules with two chlorine ions, respectively. By increasing temperature, the third step, further decomposition at range 236–550 °C for

Table 3
The magnetic moment values and electronic absorption spectral bands of ligand HL and its complexes.

Compound	*Electronic Absorption Bands $\lambda_{max.}$ (nm) in DMSO*		μ_{eff} *(B.M.)*
	Intraligand & Charge Transfer bands (nm)	d-d transitions	
Ligand HL	328 B-ring, 282 A-ring, 233, 213	–––––	–––
$[Ag(L)(H_2O)_2].\ 4H_2O$	335, 281, 225, 215	–––––	0.00
$[Y(L)(H_2O)_2\ Cl_2].\ 2H_2O$	323, 283, 210	–––––	0.00
$[Ru(L)(H_2O)_2\ Cl_2].\ 5H_2O$	333, 282, 224, 212	534	5.73

Table 4
Thermogravimetric Analyses of the Investigated Metal Complexes.

Complex	M: L	Water Elimination				Decomposition Stages (°C)	Residue (%) (metal oxide)	
		Temp. (°C) Up to	Hydrated water mass loss % Calc./Found	Temp. (°C)	Coordinated water mass loss % Calc./Found		Temp. (°C)	Calc./Found
$[Ag(L)(H_2O)_2].\ 4H_2O$	1:1	70–120	9.06 (8.95)	120–220	4.53 (4.50)	220–350 350–800	850–1000	13.55 (13.50)
$[Y(L)(H_2O)_2\ Cl_2].\ 2H_2O$	1:1	50–100	4.44 (4.40)	100–230	13.19 (13.58)	240–400 410–700	750	27.84 (27.69)
$[Ru(L)(H_2O)_2\ Cl_2].\ 5H_2O$	1:1	50–140	10.25 (10.36)	150–236	12.19 (12.26)	236–350 350–550	600	28.51 (28.35)

organic parts but at 600 °C the Ru_2O_3 is the final product remains stable as 28.51 (cal.28.35)% (Thabrew et al., 1997). The decomposition steps of all complexes are shown in Fig. 3:

The structure of the prepared naringin-metal complexes was confirmed by the spectral data and the elemental analyses and formulated as shown in Fig. 4.

3.3. In-vitro anticancer activity

To checked the Cytotoxic effect of naringin and its metal complexes [Ag(I), Y(III) and Ru (III)] were applied on human breast adenocarcinoma (MCF7) and Lung carcinoma cell line (A549). Cytotoxic effect was monitored by cell viability assay (Table 5). The pure Ag and Ru metal complexes at 100 ppm showed killing percentage against MCF7 cells reached to 100% in both metal complex with IC_{50} of 6.8 and 33.8 μg/ml respectively, and 100% against A549 cells in Ag metal complex with IC_{50} of 5.9 μg/ml and 49.3% and in Ru metal complex with IC_{50} of 89.6 μg/ml. While the pure Y metal complex at 100 ppm showed, killing percentage against A549 cells reached to 14.2% and has no potential anti-cancer effect on MCF7 cell line. Many authors showed that complexes are more effective than free flavonoids. All these data are available in various previous publications (Pereira et al., 2007;; Jun et al., 2007; Abd-El-All et al., 2013) and our obtained results in agreement with Al-Obaidi, 2014 and Abd-El-All et al., 2013). In the cytotoxic effect of flavone ligand complex against the growth of mutant mouse cells (L20B). In addition, Saadiyah et al., 2012 and El-Menshawi et al., 2010, reported that copper complexes and aqueous organum vulgare extract have a cytotoxic effect on RD cell line and attributed its cytotoxic effect to bind and cross linking of DNA which ultimately triggers apoptosis (programmed cell death).

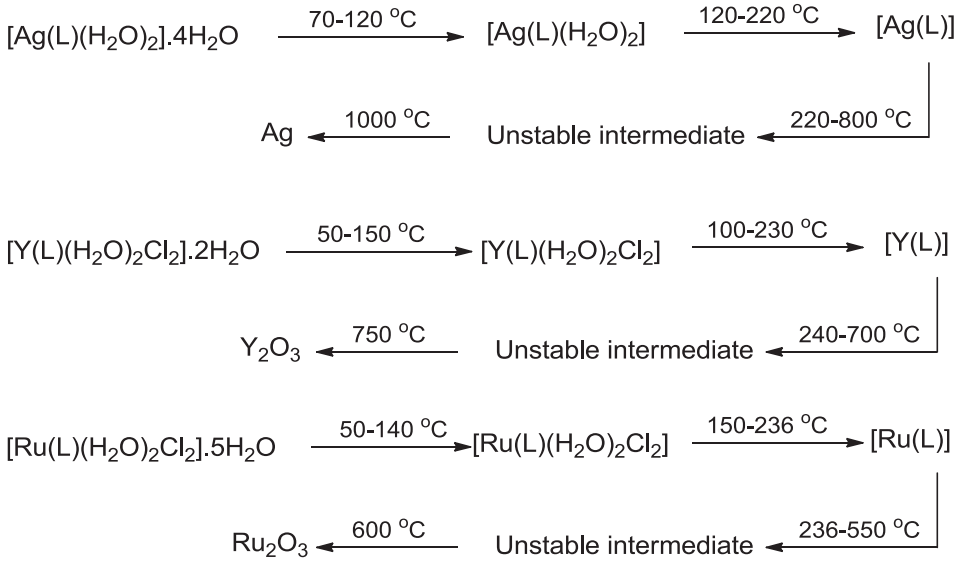

Fig. 3. The decomposition steps of the synthesized complexes.

In comparison between LC_{50} of Adriamycin used as a medical chemotherapy agent against MCF-7 and LC_{50} of Ag and Ru ligands complexes, the LC_{50} from Ag ligand complex was found higher than three times the strength of Adriamycin, while the LC_{50} of Adriamycin was slightly superior only about 30% of the Ru ligand complex. On the other hand, against A549 cell line, the LC_{50} from Ag ligand complex was found higher than four times the strength of Adriamycin, while, the Adriamycin compound was superior more than twice the strength of the Ru ligand complex. In this regard, it has clearly demonstrated that copper (II)-naringin complex activity is higher as anti-inflammatory and antioxidant compared to free naringin. All data obtained through UV–VIS and FT-IR suggest that the systematization of Cu (II) transition metal is in positions 4 and 5 of the naringin intensive ring, and the increase in biological activity of complex could be correlate to the coordination of Cu (II) in this position (Pereira et al., 2007).

4. Conclusions

In this work the naturally isolated Naringin (**HL**) combined with transition metal ions [Ag (I), Y (III) and Ru (III)] are characterized by FT-IR, UV–VIS, elemental analysis, molar conductance, magnetic properties and TGA. Transition metal ions increase the activity of naringin when they are coordinated to each other. Cytotoxic effects of the synthesized compounds were checked for anticancer activity and successfully applied adenocarcinoma (MCF7) and Lung carcinoma cell line (A549) using cell viability assay. The results announce the enhanced activity of most **L**-metal complexes over the free **HL**. LC50 of Ag ligand complex demonstrated strong cytotoxicity against MCF-7 and A549 cell line that was found higher active more than three and four times the strength, respectively when compared to LC50 of Adriamycin. While LC50 of Adriamycin compound was slightly more active only about 30% and twice the strength of the Ru ligand complex

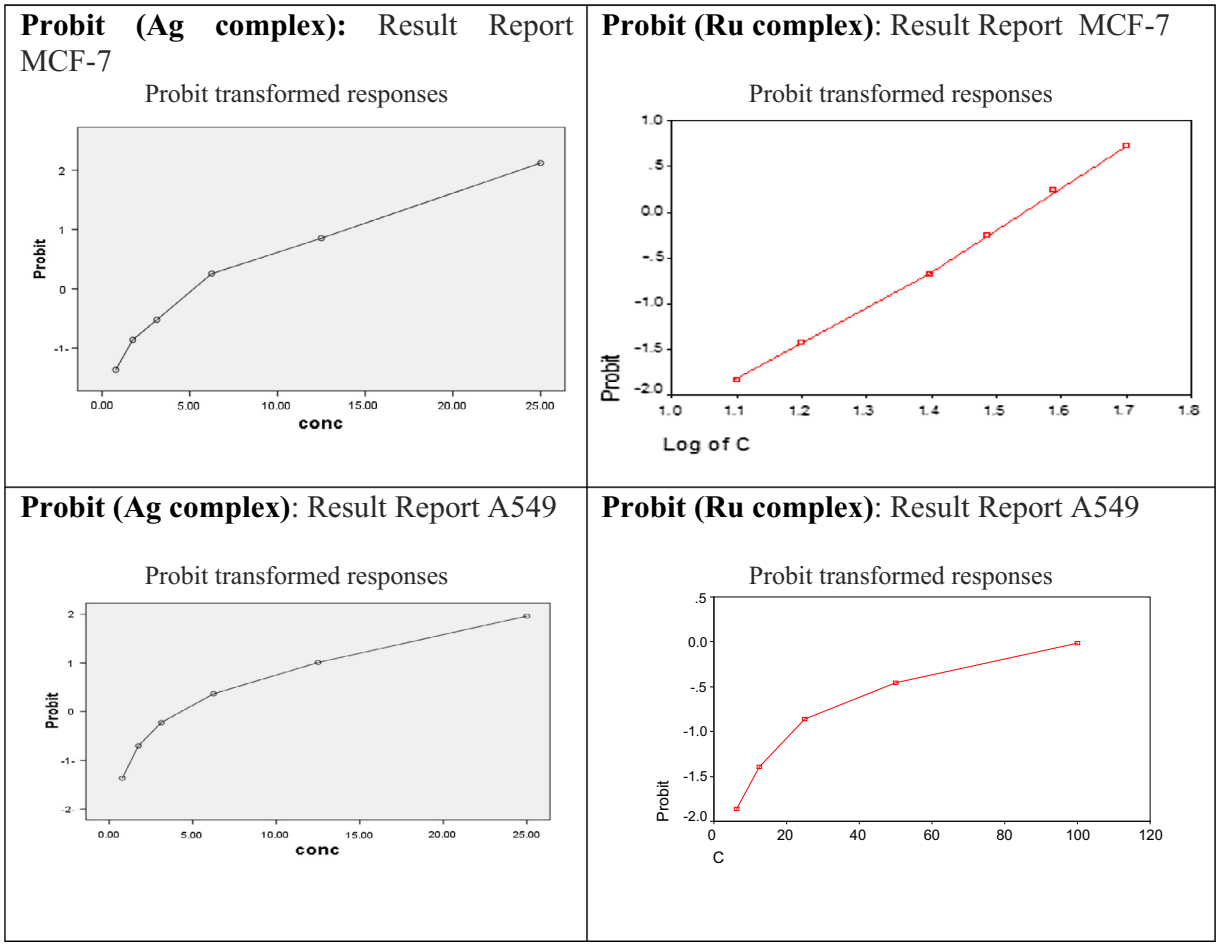

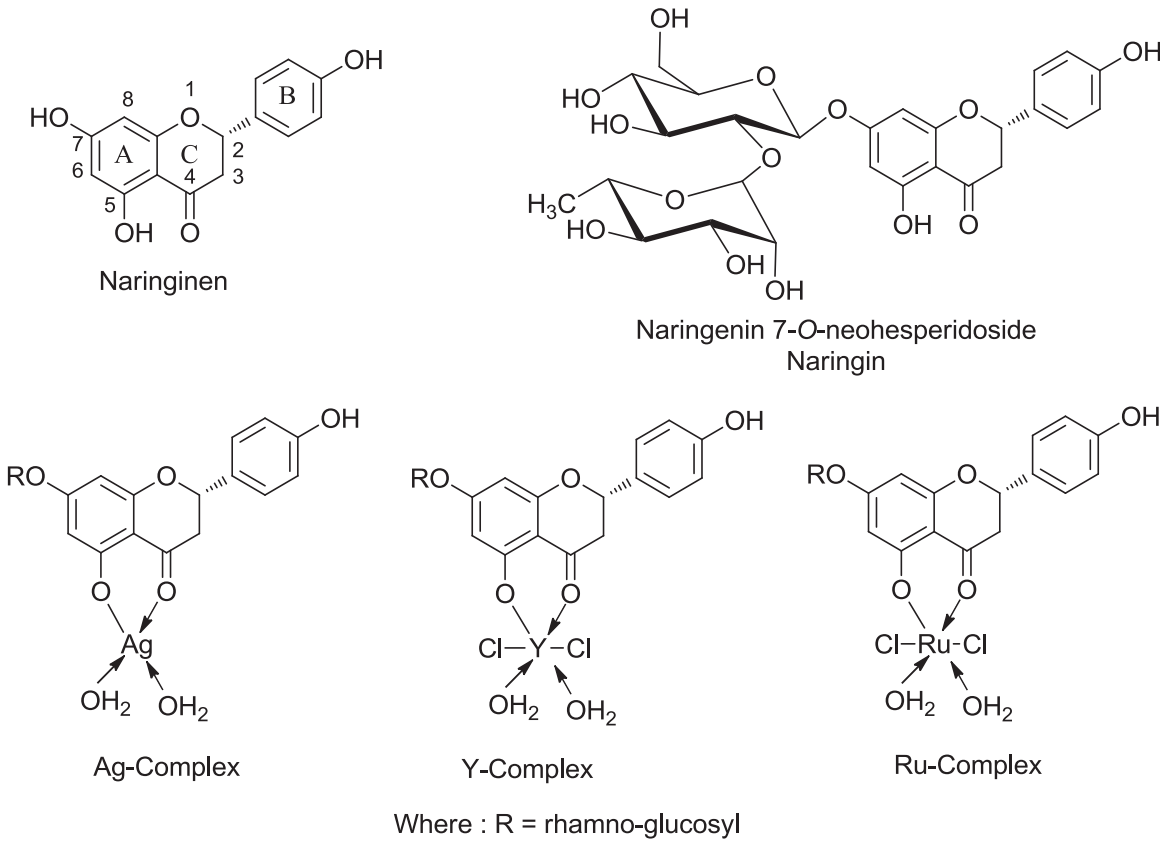

Fig. 4. The suggested structural formulae of the Complexes.

Table 5
Effect of naringin and its complexes on MCF-7 and A549 cell line.

Lung carcinoma cell line (A549)	Human Caucasian breast adenocarcinoma (MCF-7)			Lung carcinoma cell line (A549)		
	LC_{50} (μg/ml)	LC_{90} (μg/ml)	% Remarks at 100 ppm	LC_{50} (μg/ml)	LC_{90} (μg/ml)	% Remarks at 100 ppm
Naringin (authentic sample)	–––	–––––	–––––	–––––	–––	––
Isolated Naringin HL	–––	–––––	–15	–––––	–––	12.3
[Ag(**L**)$(H_2O)_2$]. $4H_2O$	6.8	12.6	100	5.9	14.8	100
[Y(**L**)$(H_2O)_2$ Cl_2]. $2H_2O$	–––	–––––	–19	–––––	–––––	14.2
[Ru(**L**)$(H_2O)_2$ Cl_2].$5H_2O$	33.8	63.3	100	89.6	153	49.3
Adriamycin (Doxorubicin)	26.1	45.02	100	28.3	48.8	100
DMSO	–––	–––	3	–––	–––	5
Negative control	–––	–––	–––––	–––	–––––	0

LC_{50}: Lethal concentration of the sample which causes the death of 50% of cells in 48 hrs.; LC_{90}: Lethal concentration of the sample which causes the death of 90% of cells in 48 hrs.

against MCF-7 and A549 cell line, respectively. It is known that the high rate of metastasis associated to the fact that these cells frequently display multidrug resistance, make the treatment of metastatic disease difficult, so, we think our results about Ag and Ru Complex are very good in this direction as an addition to a range of new drugs.

Acknowledgments

The authors would like to thank the Deanship of Scientific Research (DSR) at Jazan University for the financial support for this work (Grant No 00142/7/37).

References

Abd-El-All, A.S., Ammar, A.L., Mousa, H.A., Bassyouni, F.A., Hegab, K.H., El-Hashash, M.A., Atta-Allah, S.R., Abd El-Hady, W.H., Osman, S.A.M., 2013. Synthesis of Ag (I), Cu(II), La(III) complexes of some newmannich bases incorporating 1,2,4-triazine moiety and studying their antihypertensive and diuretic activities. J. Appl. Sci. Res. 9 (1), 469–481.

Afanasév, I.B., Ostrakhovitchm, E.A., Mikhal Chik, E.V., Ibraginova, G.A., Korkina, L.G., 2001. Enhancement of antioxidant and anti-inflammatory activities of bioflavonoid rutin by complexation with transition metals. Biochem. Pharmacol. 61, 677–684.

Agrawal, S., 2015. Drug -metal complexes in research – a review. Ultra Scientist 27 (2)B, 113–116.

Al Hassani, R.A., Nife, O., Ayad, T.M., 2015. Synthesis, characterization, theoretical studies and biological activities of naringin metal cnplexes. Acta Chim. Pharm. Indica 5 (3), 129–142.

Al Hassani, R.A., Nife, O., Ayad, T.M., Adil, A.A., 2016. Synthesis, characterization, theoretical studies and biological activities of naringin metal complexes. ICAIJ 11 (2), 47–57.

Al-Obaidi, O.H., 2014. Study of the cytotoxicity effect of new Cu (II) And Ni (II) complexes of flavon on Cancer (Cell Line L20b) and antimicrobial activity. Intl. Res. J. Appl. Basic Sci. 8 (5), 540–544.

Pöthig, Alexander, Ahmed, Sara, Cecilie Winther-Larsen, Hanne, Guan, Shengyang, Altmann, Philipp J., Kudermann, Jürgen, Andresen, Adriana Magalhães Santos, Gjøen, Tor, Høgmoen Åstrand, Ove Alexander, 2018. Antimicrobial activity and cytotoxicity of Ag(I) and Au(I) pillarplexes. Front. Chem. V. 6, A 584.

Ejidike, I.P., Ajibade, P.A., 2016. Ruthenium (III) complexes of heterocyclic tridentate (ONN) schiff base: synthesis, characterization and its biological properties as an antiradical and antiproliferative agent. Int. J. Mol. Sci. 17, 60–68.

El-Menshawi, B.S., Fayad, W., Mahmoud, K., El-Hallouty, S.M., El-Manawaty, M., Olofsson, M.H., Linder, S., 2010. Screening of natural products for therapeutic activity against solid tumors. Indian J. Exp. Biol. 48, 258–264.

Corrêa, R.S., da Silva, M.M., Graminha, A.E., Meira, C.S., Santos, J.A., Moreira, D.R., Soares, M.B., Von Poelhsitz, G., Castellano, E.E., Bloch Jr, C., Cominetti, M.R., Batista, A.A., 2016. Ruthenium (II) complexes of 1,3-thiazolidine-2-thione: Cytotoxicity against tumor cells and anti-Trypanosoma cruzi activity enhanced upon combination with benznidazole. J. Inorg. Biochem. 156, 153–163.

Ghazanfar, S.A., 1994. Handbook of Arabian medicinal plants. CRC Press, Boca Raton.

Gorinstein, S., Huang, D., Leontowicz, H., Leontowicz, M., Yamamoto, K., Soliva-Fortuny, R., Martin Belloso, O., Martinez Ayala, A.L., Trakhtenberg, S., 2006. Determination of naringin and hesperidin in citrus fruit by high-performance liquid chromatography. The antioxidant potential of citrus fruit. Acta Chromatogr. 17, 108–124.

Hynes, M.J., O'Coinceanainn, M., 2004. The kinetics and mechanisms of reactions of iron (III) with caffeic acid, chlorogenic acid, sinapic acid, ferulic acid and naringin. J. Inorg. Biochem. 98 (8), 1457–1464.

Ibrahim, E.M., Zeeneldin, A.A., Sadiq, B.B., Ezzat, A.A., 2008. The present and the future of breast cancer burden in the Kingdom of Saudi Arabia. Med. Oncol. 25 (4), 387–393.

Jun, T., Bochu, W., Liancai, Z., 2007. Hydrolytic cleavage of DNA by quercetin zinc (II) complex. Bioorg. Med. Chem. Lett. 17, 1197–1199.

Kanaze, F.I., Gabrieli, C., Kokkalou, E., Georgarakis, M., Niopas, I., 2003. Simultaneous reversed-phase high-performance liquid chromatographic method for the determination of diosmin, hesperidin and naringin in different citrus fruit juices and pharmaceutical formulations. J. Pharm. Biomed. Anal. 33 (2), 243–249.

Knoll, J.D., Turro, C., 2015. Control and utilization of ruthenium and rhodium metal complex excited states for photo activated cancer therapy. Coord. Chem. Rev. 282, 110–126.

Lucilene, D.M., Regina, M.S.P., Alexandra, C.H.F.S., Marcos, N.E., Lauro, T.K., 2007. Electrochemical and spectroscopic characterization of the interaction between DNA and Cu(II)-naringincomplexe. J. Pharam. Biomed. Anal. 45, 706–713.

Mabry, T.J., Markham, K.R., Thomas, M.B., 1970. The systematic identification of flavonoids. Springer, New York, p. 354.

Mello, L.D., Pereira, R.M.S., Sawaya, A.C.H.F., Eberlin, M.N., Kubota, L.T., 2007. Electrochemical and spectroscopic characterization of the interaction between DNA and Cu(II)–naringin complex. J. Pharm. Biomed. Anal. 45 (5), 706–713.

Mosmann, T., 1983. Rapid colorimetric assays for cellular growth and survival: application to proliferation and cytotoxicity assays. J. Immunol. Methods 65, 55–63.

Munde, S.A., Amarnath, N.J., Sarika, M.J., Trimbak, K.C., 2010. Synthesis, characterization and thermal study of some transition metal complexes of an asymmetrical tetradentate Schiff base ligand. J. Serb. Chem. Soc. 75 (3), 349–359.

Obasi, L.N., Oruma, U.S., Al-Swaidan, I.A., Ramasami, P., Ezeorah, C.J., Ochonogor, A. E., 2017. Synthesis, characterization and antibacterial studies of N-(Benzothiazol-2-yl)-4-chlorobenzenesulphonamide and Its neodymium(III) and thallium(III) complexes. Molecules 22, 153.

Pereira, R.M.S., Andrades, N.E.D., Paulino, N., Sawaya, A.C.H.F., Eberlin, M.N., Marcucci, M.C., Favero, G.M., Novak, E.M., Bydlowski, S.P., 2007. Synthesis and characterization of a metal complex containing naringin and Cu, and its antioxidant, antimicrobial, anti-inflammatory and tumor cell cytotoxicity. Molecules 12, 1352–1366.

Regina, M.S.P., Norma, E.D.A., Niraldo, P., Alexandra, C.H.F.S., Marcos, N.E., Marcucci, M.C., Giovani, M.F., Novak, E.M., Bydlowski, S.P., 2007. Synthesis and characterization of a metal complex containing naringin and Cu, and its antioxidant, antimicrobial, anti-inflammatory and tumor cell cytotoxicity. Molecules 12, 1352–1366.

Rout, S.S., Sahoo, R.N., Pattanaik, S., Pal, A., Si, S.C., Mohanty, P., 2013. Anti-nociceptive activities of complexes of naringin with Co (II) metal ions. Int. J. Pharm. Pharm. Sci. 5 (3), 972–975.

Saadiyah, A.D., Jinan, H., Iman, H.J., 2012. Study of the cytotoxic effect of new copper (II) complexes and aqueous extract of *Origanum Vulgare* L. plant on cancer cell Line (RD). J. Al-Nahrain Univ. 15 (2), 23–28.

Sing, R., Gupta, N., Fahmi, N., 1999. Biochemical aspects of dioxomolybdenum (VI) and manganese (II) complexes. Indian J. Chem. 38, 1150–1158.

Sudhanshu, S.R., Rudra, N.S., Sovan, P., Abhisek, P., Sudam, C.S., Prakash, M., 2013. Anti-Nociceptive activities of complexes of naringin with CO (II) Metal Ions. Int. J. Pharm. Sci. 5 (3), 972–975.

Sudto, K., Surachai, P., Supason, W., 2009. An efficient method for the large scale isolation of naringin from pomelo (*Citrus grandis*) peel. Int. J. Food Sci. Technol. 44 (9), 1737–1742.

Thabrew, M.I., Hughes, R.D., McFarlane, I.G., 1997. Screening of hepatoprotective plant components using a HepG2 cell cytotoxicity assay. J. Pharm. Pharmacol. 49, 1132–1135.

Vasile Scăeţeanu, G., Chifiriuc, M.C., Bleotu, C., Kamerzan, C., Măruţescu, L., Daniliuc, C.G., Maxim, C., Calu, L., Olar, R., Badea, M., 2018. Synthesis, structural characterization, antimicrobial activity, and in vitro biocompatibility of new unsaturated carboxylate complexes with 2,2′-bipyridine. Molecules 23, 157.

Vishnu Varthan, V.J., Srividya, A.R., Sathish Kumar, M.N., 2013. Role of naringin and naringenin in various diseased conditions - a review. Int. J. Pharm. Res. Scholars 2 (4), 198–212.

Zhang, J., Brodbelt, J.S., 2005. Silver complexation and tandem mass spectrometry for differentiation of isomeric flavonoid diglycosides. Anal. Chem. 77, 1761–1770.